

## Dendritic Molecular Capsules for Hydrophobic Compounds

Meredith T. Morgan, Michael A. Carnahan, Chad E. Immoos, Anthony A. Ribeiro,<sup>†</sup>  
Stella Finkelstein, Stephen J. Lee,<sup>‡</sup> and Mark W. Grinstaff\*

*Contribution from the Departments of Chemistry and Biomedical Engineering,  
Boston University, Boston, Massachusetts 02215 and Departments of Chemistry and  
Biomedical Engineering, Duke University, Durham, North Carolina 27708*

Received February 18, 2003; E-mail: mgrin@bu.edu

**Abstract:** Reichardt's dye, a highly solvatochromic dye, was encapsulated within poly (glycerol succinic acid) ([Gn]-PGLSA-OH) dendrimers to investigate the interior environment of these dendritic macromolecules. The absorption maximum for the encapsulated Reichardt's dye in water was indicative of a relatively high dielectric constant present within the dye/dendrimer complex. <sup>1</sup>H NMR of the encapsulated complex showed the presence of aromatic protons from Reichardt's dye along with the aliphatic protons of the dendrimer. Additionally, there were substantial changes in *T*<sub>1</sub> and *T*<sub>2</sub> times of the encapsulated dye when compared with the free dye, and <sup>1</sup>H NOESY spectra for the complex showed a significant number of intermolecular NOE cross-peaks. These data reveal the close through-space proximity of the dye to the dendrimer and the restricted motion of the encapsulated dye. To demonstrate the potential use of these macromolecules as drug delivery vehicles, the poorly water-soluble anticancer drug 10-hydroxycamptothecin (10HCPT) was encapsulated within a carboxylated PGLSA dendrimer ([G4]-PGLSA-COONa). Cytotoxicity assays with human breast cancer cells showed a significant reduction of cell viability, demonstrating that 10HCPT retains activity upon encapsulation.

### Introduction

Dendrimers are highly branched, well-defined monodisperse macromolecules composed of a focal point, interior region, and numerous end groups.<sup>1–18</sup> As the dendrimer generation increases, the macromolecule adopts a globular shape, and the end groups strongly influence the properties of the dendrimer.

When compared to similar conventional linear polymers, dendrimers possess significantly different physical and chemical properties including solubility, chemical reactivity, viscosity, and glass-transition temperature.<sup>10–12,19</sup> Moreover, the three-dimensional structure and material properties of dendrimers can be tailored through specific chemical alterations. Given these unique characteristics, dendrimers are of interest for chemical and biomedical applications. We are investigating dendrimers composed of biocompatible monomers (e.g., glycerol, lactic acid, and succinic acid), termed "biodendrimers."<sup>20–23</sup> Basic studies with these macromolecules will provide new insights and directions for the use of dendritic polymers in medicine.

Two current challenges in drug delivery are targeting specific biological sites and administering hydrophobic drugs.<sup>24–26</sup> The latter is important because a large number of highly active pharmaceuticals lack appreciable water solubility. Therefore, these drugs are either not clinically used, delivered in large volumes of aqueous solution, delivered in conjunction with surfactants (e.g., Cremophore EL), or chemically derivatized to afford soluble prodrugs: all of which can result in reduced efficacy or harmful side effects. Approaches to delivering

<sup>†</sup> Duke NMR Spectroscopy Center and Department of Radiology, Duke University, Durham, NC 27708.

<sup>‡</sup> Army Research Office, RTP, NC 27709.

- (1) Bosman, A. W.; Janssen, H. M.; Meijer, E. W. *Chem. Rev.* **1999**, *99*, 1665–1688.
- (2) Zeng, F.; Zimmerman, S. C. *Chem. Rev.* **1997**, *97*, 1681–1712.
- (3) Fischer, M.; Vögtle, F. *Angew. Chem., Int. Ed. Engl.* **1999**, *38*, 884–905.
- (4) Majoral, J. P.; Caminade, A. M. *Chem. Rev.* **1999**, *99*, 845–880.
- (5) Mathews, O. A.; Shipway, A. N.; Stoddart, J. F. *Prog. Polym. Sci.* **1998**, *23*, 1–56.
- (6) Newkome, G. R.; Moorefield, C. N.; Keith, J. N.; Baker, G. R.; Escamilla, G. H. *Angew. Chem., Int. Ed. Engl.* **1994**, *106*, 701–703.
- (7) Issberner, J.; Moors, R.; Vögtle, F. *Angew. Chem., Int. Ed. Engl.* **1994**, *33*, 2413–2420.
- (8) Vögtle, F. *Dendrimers I*; Springer: Berlin; Vol. 197.
- (9) Vögtle, F. *Dendrimers II: Architecture, Nanostructure, and Supramolecular Chemistry*; Springer: Berlin; Vol. 210.
- (10) Vögtle, F. *Dendrimers III: Design, Dimension, Function*; Springer: Berlin, 2001; Vol. 212.
- (11) Newkome, G. R.; Moorefield, C. N.; Vögtle, F. *Dendritic Molecules: Concepts, Synthesis, Perspectives*; VCH: New York, 1996.
- (12) Fréchet, J. M. J.; Tomalia, D. A. *Dendrimers and Other Dendritic Polymers* Chichester, UK, 2001.
- (13) Fréchet, J. M. J. *Proc. Natl. Acad. Sci.* **2002**, *99*, 4782–4787.
- (14) Buhleier, W.; Wehner, F. V.; Vögtle, F. *Synthesis* **1987**, 155–158.
- (15) Hawker, C. J.; Fréchet, J. M. J. *J. Am. Chem. Soc.* **1990**, *112*, 2, 7638–7647.
- (16) Tomalia, D. A.; Baker, H.; Dewald, J.; Hall, M.; Kallos, G.; Martin, S.; Roeck, J.; Ryder, J.; Smith, P. *Polym. J.* **1985**, *17*, 117–132.
- (17) Tomalia, D. A.; Baker, H.; Dewald, J.; Hall, M.; Kallos, G.; Martin, S.; Roeck, J.; Ryder, J.; Smith, P. *Macromolecules* **1986**, *19*, 2466–2468.
- (18) Newkome, G. R.; Yao, Z.; Baker, G. R.; Gupta, V. K. *J. Org. Chem.* **1985**, *50*, 2003–2004.

- (19) Harth, E.; Hecht, S.; Helms, B.; Malmstrom, E.; Fréchet, J. M. J.; Hawker, C. J. *Am. Chem. Soc.* **2002**, *124*, 3926–3938.
- (20) Carnahan, M. A.; Grinstaff, M. W. *J. Am. Chem. Soc.* **2001**, *123*, 2905–2906.
- (21) Carnahan, M. A.; Grinstaff, M. W. *Macromolecules* **2001**, *34*, 7648–7655.
- (22) Carnahan, M. A.; Middleton, C.; Kim, J.; Kim, T.; Grinstaff, M. W. *J. Am. Chem. Soc.* **2002**, *124*, 5291–5293.
- (23) Grinstaff, M. W. *Chem. Eur. J.* **2002**, *8*, 2838–2846.
- (24) Kopeček, J. *Polym. Med.* **1977**, *7*, 191–221.
- (25) Langer, R. *Nature* **1998**, *392*, 5–10.
- (26) Uhrich, K. E.; Cannizzaro, S. M.; Langer, R.; Shakesheff, K. M. *Chem. Rev.* **1999**, *99*, 3181–3198.

hydrophobic compounds using polymeric carriers, such as dendrimers,<sup>27–33</sup> are being explored in many laboratories. In previous studies, rose bengal<sup>34</sup> and acetylsalicylic acid<sup>35</sup> were noncovalently encapsulated within poly(propylene imine) and poly(amido amine) dendrimers. In the case of rose bengal encapsulated within Meijer's dendritic box, the internalized dye molecules were confined within the dendrimer as a consequence of steric congestion at the dendrimer periphery.<sup>34</sup> Pyrene was encapsulated within both poly(propylene imine) dendrimers and unimolecular micelles based on pegylated Fréchet-type dendrimers.<sup>36,37</sup> Additionally, fluorescent dyes such as phenol blue<sup>38</sup> and 4-(dicyanomethylene)-2-methyl-6-(4-dimethylaminostyryl)-4H-pyrene (DCM),<sup>39</sup> have been encapsulated. Fluorescence self-quenching is reduced, as the dyes are isolated from one another. A large internal pocket was also created in a porphyrin-based dendrimer through cross-linking the peripheral end groups and then hydrolyzing the ester bonds between the dendritic arms and the internal porphyrin core. This dendrimer was subsequently capable of selectively binding a guest porphyrin molecule.<sup>40</sup> We report the encapsulation of a solvatochromic dye within a poly(glycerol-succinic acid) (PGLSA) dendrimer and the subsequent characterization of this supramolecular assembly using UV-vis and various 1D and 2D NMR experiments. Additionally, we encapsulated a hydrophobic anticancer drug and demonstrated that cytotoxicity was retained in the presence of human breast cancer cells.

## Results and Discussion

Dendrimers are synthesized through either a convergent (periphery to core) or divergent (core to periphery) synthesis. For experiments described herein, a generation four (G4) PGLSA dendrimer (**1**) was synthesized in a divergent manner by successive esterifications with 2-(*cis*-1,3-*O*-benzylidene-glycerol)succinic acid mono ester and deprotections (hydrogenolysis) with H<sub>2</sub>/Pd/C.<sup>21</sup> The hydroxyl (OH) and carboxylate (COONa) terminated dendrimers with molecular weights of 10 715 and 18 500, respectively, were fully characterized by NMR, MALDI TOF mass spectrometry, SEC, and quasi-elastic light scattering.

The strongly solvatochromic Reichardt's dye (2,6-diphenyl-4-(2,4,6-triphenylpyridinio)phenolate (**3**) Figures 1 and 3, M<sub>w</sub> = 552 g/mol) was encapsulated within the [G4]-PGLSA-OH dendrimer. This solvatochromic dye has been used previously to create the empirical E<sub>T</sub>(30) solvent polarity scale and was

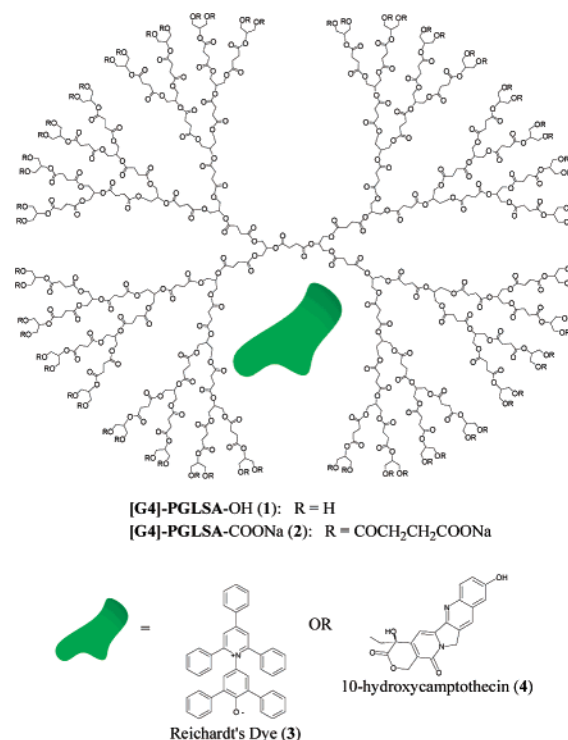


Figure 1. [G4]-PGLSA biodendrimers and encapsulants.

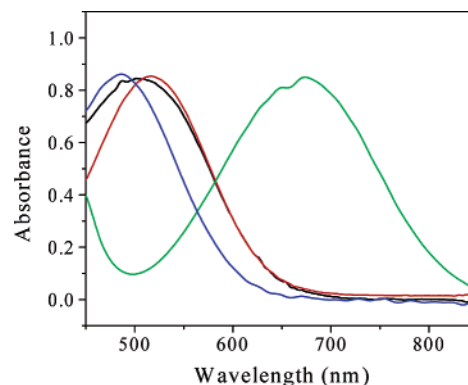


Figure 2. UV-vis data for Reichardt's dye in Acetone (green), MeOH (blue), encapsulated in [G4]-PGLSA-OH (black), and 60:40 H<sub>2</sub>O:MeOH (red).

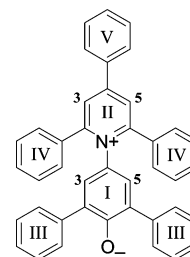


Figure 3. Structure of Reichardt's E<sub>T</sub>(30) dye with proton and ring assignments.

also used to study micelle/solution interfaces, phospholipid bilayers, microemulsions, and polymer mixtures.<sup>41</sup> Encapsulation of Reichardt's dye within G3 and G4 PGLSA dendrimers was investigated; the G2 dendrimer did not encapsulate the dye. This observation is consistent with the globular structure required for encapsulation by a dendrimer. The G3 dendrimer encapsu-

- (27) Schultz, L. G.; Zimmerman, S. C. *Pharm. News* **1999**, 6, 25–29.  
(28) Liu, H.; Farrell, S.; Uhrich, K. E. *J. Controlled Release* **2000**, 68, 167–174.  
(29) Liu, M.; Kono, K.; Fréchet, J. M. J. *J. Controlled Release* **2000**, 65, 121–131.  
(30) Malik, N.; Wimattapatapee, R.; Klopsch, R.; Lorenz, K.; Frey, H.; Weener, J. W.; Meijer, E. W.; Paulus, W.; Duncan, R. *J. Controlled Release* **2000**, 65, 133–148.  
(31) Esfand, R.; Tomalia, D. A. *Drug Discovery Today* **2001**, 6, 427–436.  
(32) Kim, Y. H.; Webster, O. W. *J. Am. Chem. Soc.* **1990**, 112, 4592–4593.  
(33) Newkome, G. R.; Moorefield, C. N. *Angew. Chem., Int. Ed. Engl.* **1991**, 30, 1178–1180.  
(34) Jansen, J. G. F. A.; Drabander-van den Berg, E. M. M.; Meijer, E. W. *Science* **1994**, 266, 1226–1229.  
(35) Naylor, A.; Goddard, W.; Kiefer, G.; Tomalia, D. *J. Am. Chem. Soc.* **1989**, 111, 2339–2341.  
(36) Pistolis, G.; Malliaris, A. *Langmuir* **2002**, 18, 246–251.  
(37) Hawker, C. J.; Wooley, K. L.; Fréchet, J. M. J. *J. Chem. Soc., Perkin Trans. 1* **1993**, 1287–1297.  
(38) Richter-Egger, D.; Tesfai, A.; Tucker, S. *Anal. Chem.* **2001**, 73, 5743–5751.  
(39) Yokoyama, S.; Otomo, A.; Mashiko, S. *Appl. Phys. Lett.* **2002**, 80, 7–9.  
(40) Zimmerman, S.; Wednland, M.; Rakow, N.; Zharov, I.; Suslick, K. *Nature* **2002**, 418, 399–403.

- (41) Reichardt, C. *Chem. Rev.* **1994**, 94, 2319–2358.

**Table 1.** Absorbance Maxima and  $E_T(30)$  Values for Reichardt's Dye in Solvents of Varying Polarities.<sup>42</sup> Sodium Dodecanoate (SDDC)<sup>43</sup>

solvent	absorbance (nm)	$E_T(30)$
water	453	63.1
glycerol	502	57.0
SDDC <sup>43</sup>	504	56.7
methanol	516	55.4
acetone	677	42.2
ethyl acetate	750	38.1

lated a maximum of  $\sim 1$  dye molecule per dendrimer. Various ratios of Reichardt's dye ranging from 0.5 to 2.0 were encapsulated within the G4 dendrimer.<sup>42</sup> The maximum number of dye molecules encapsulated within the G4 dendrimer was approximately two,<sup>43</sup> affording a concentration of 4.7 mM, a 200-fold improvement of the dye solubility in water without dendrimer (2.0  $\mu$ M). The same encapsulation procedure was attempted with a generation 4.5 PAMAM carboxylate terminated dendrimer, but no appreciable amount of Reichardt's dye was encapsulated. We suspect the poor encapsulation efficiency with the PAMAM dendrimer is a consequence of the cationic character of the dendrimer.

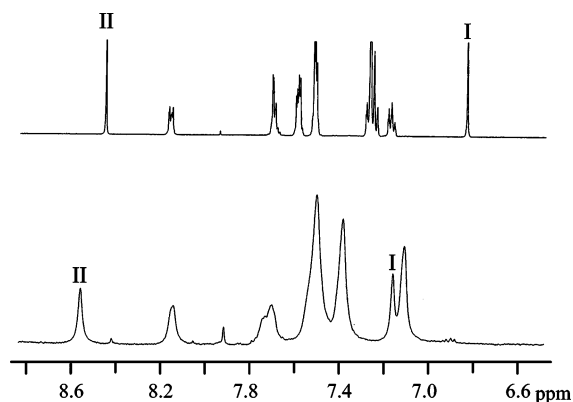
UV-vis experiments showed the expected solvatochromic shift for Reichardt's dye, with a blue shift in the absorbance maximum as the solvent polarity increased (Figure 2 and Table 1). The UV-vis spectrum of [G4]-PGLSA-OH encapsulated Reichardt's dye shows a  $\lambda_{max}$  at 503 nm, yielding an  $E_T(30)$  of 56.8. This absorbance wavelength indicates the presence of an apparent high dielectric constant in the interior of the dendrimer. The  $E_T(30)$  value for the encapsulated dye is between methanol (55.3) and water (63.1), similar to the value for glycerol (57.0), but significantly different from acetone (42.2), ethyl acetate (38.1), and hexanes (31.0).<sup>44</sup> The interior environment of the dendrimer is less polar than water and approximates the polarity of glycerol. As Reichardt's dye is only slightly water soluble, it has been used to measure the effective dielectric constant at aqueous micellar interfaces. This interface is highly hydrated in the anionic surfactant, sodium dodecanoate (SDDC), with an  $E_T(30)$  of 56.7.<sup>45</sup> The relatively high  $E_T(30)$  for the dendrimer interior can also be rationalized by the penetration of water molecules within this supramolecular assembly to afford a highly hydrated state.

The hydrodynamic radius ( $R_h$ ) of the [G4]-PGLSA-OH dendrimer in H<sub>2</sub>O was determined using quasi-elastic light scattering (QELS). The average hydrodynamic radius of the [G4]-PGLSA-OH dendrimer was found to be 7 nm. Upon encapsulation of Reichardt's dye, the hydrodynamic radius of the dendrimer in H<sub>2</sub>O decreased to 4 nm. The reduction in hydrodynamic radius suggests that the aliphatic dendrimer collapsed around the dye. The hydrodynamic radius of the [G4]-PGLSA-OH dendrimer was solvent dependent. In methanol, the  $R_h$  was 3 nm, whereas in 1:1 CH<sub>3</sub>CN:H<sub>2</sub>O, and THF the  $R_h$  was greater than 30 nm. The apparent large hydrodynamic radius of the dendrimer indicates the likely formation of aggregates in solution.

**Table 2.** <sup>1</sup>H NMR Chemical Shifts (ppm),  $T_1$  and  $T_2$  Relaxation Time Constants (sec) for Free Reichardt's Dye (CD<sub>3</sub>OD) and Reichardt's Dye Encapsulated within [G4]-PGLSA-OH (D<sub>2</sub>O)<sup>a</sup>

ring	protons	$\delta_{TMS}$ (free)	$T_1$ (free)	$T_2$ (free)	$\delta_{DSS}$ (encapsulated)	$T_1$ (encapsulated)	$T_2$ (encapsulated)
I	meta	6.738(s)	1.81	1.44	7.184(s)	0.715	0.022
II	meta	8.392(s)	1.62	1.28	8.603(s)	0.738	0.021
III	ortho	7.206(m)	1.78	0.321	7.392(m)	0.674	0.022
	meta	7.181(m)	1.70	0.505	7.113(m)	0.686	0.024
IV	para	7.107(m)	1.97	0.8.03			
	ortho	7.513(m)	1.72	0.471	7.529(m)	0.679	0.018
	meta	7.438(m)	1.60	0.264			
V	para	7.430(m)					
	ortho	8.103(m)	1.62	0.021	8.185(m)	0.750	0.012
	meta	7.638(m)	1.85	0.027	7.724(m)	0.728	0.019
	para	7.643(m)			7.759(m)		

<sup>a</sup> Shifts in CD<sub>3</sub>OD were measured relative to an internal TMS standard and shifts in D<sub>2</sub>O were measured relative to an internal DSS standard.

**Figure 4.** <sup>1</sup>H NMR for (top) Reichardt's dye in CD<sub>3</sub>OD and (bottom) [G4]-PGLSA-OH encapsulated Reichardt's dye in D<sub>2</sub>O.

To gain further insight into the nature of the encapsulated dye-dendrimer interaction, we performed a series of 1D and 2D NMR experiments. Full <sup>1</sup>H NMR assignments for free Reichardt's dye (in CD<sub>3</sub>OD) and encapsulated within [G4]-PGLSA-OH (in D<sub>2</sub>O) were derived from COSY experiments (Table 2).<sup>46</sup> The <sup>1</sup>H NMR spectrum of the [G4]-PGLSA-OH encapsulated dye reveals significant chemical shifts, line shape changes, and substantial line broadening of the aromatic protons compared to free Reichardt's dye (Figure 4). The singlet resonances from rings I and II of the free dye resonate at 8.39 and 6.73 ppm and shift downfield to 8.60 and 7.18 ppm when encapsulated within [G4]-PGLSA-OH. In the absence of dendrimer, the ortho and meta protons of ring III correspond to the multiplet (8 protons) at 7.20 ppm and the para protons correspond to the multiplet (2 protons) at 7.10 ppm. When the dye is encapsulated within the dendrimer, the meta protons shift upfield to 7.10 ppm and the ortho protons overlap the signal from the para protons at 7.40 ppm. In free Reichardt's dye, the 7.51 ppm multiplet (4 protons) arises from the ortho protons of ring IV and the meta and para protons correspond to the multiplet (6 protons) at 7.43 ppm. These resonances merge into a 10 proton multiplet near 7.53 ppm upon encapsulation. For Reichardt's dye in the absence of dendrimer, the ortho protons of ring V resonate at 8.10 ppm (2 protons) and the multiplet at 7.64 ppm (3 protons) corresponds to the meta and para protons

(42) UV-vis spectra for various ratios of encapsulated Reichardt's dye in [G4]-PGLSA-OH are available in the SI (SI Figure 4).

(43) See figure in the SI.

(44) Reichardt, C. *Solvents and Solvent Effects in Organic Chemistry*, 2nd ed.; VCH: Weinheim, Germany, 1988.

(45) Zachariasse, K.; Phuc, N.; Kozankiewicz, B. *J. Phys. Chem.* **1981**, *85*, 2676–2683.

(46) <sup>1</sup>H COSY for both the encapsulated and free Reichardt's dye are shown in the SI (SI Figures 1 and 2).

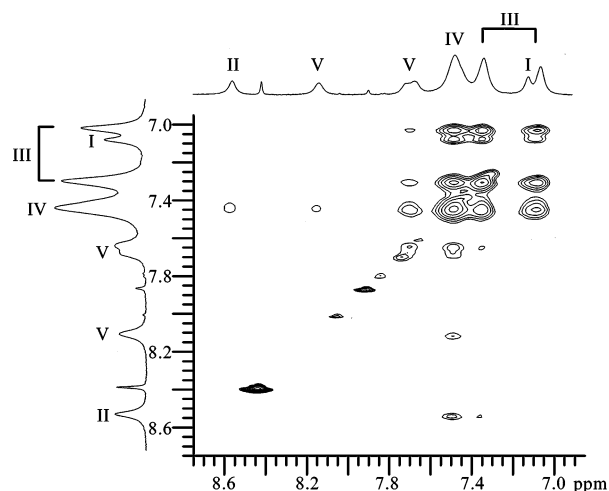


**Figure 5.** Aromatic expansion of  $^1\text{H}$  NMR NOESY of [G4]-PGLSA-OH encapsulated Reichardt's dye in  $\text{D}_2\text{O}$ .

of ring V. When the dye is encapsulated, these signals shift to 8.18 and 7.74 ppm, respectively.<sup>46</sup>

The  $^1\text{H}$  NMR spin–lattice relaxation time constants ( $T_1$ ) for the protons of ring I and ring II for free Reichardt's dye (in  $\text{CD}_3\text{OD}$ ) decrease from 1.8 and 1.6 s to 0.71 and 0.74 s when encapsulated within the [G4]-PGLSA-OH dendrimer (in  $\text{D}_2\text{O}$ ). Spin–spin relaxation time measurements revealed that the  $T_2$  of these singlets also decreased from 1.44 and 1.28 s for the free dye (in  $\text{CD}_3\text{OD}$ ) to 0.022 and 0.021 s, respectively, when encapsulated within the dendrimer (in  $\text{D}_2\text{O}$ ). The large decrease in  $T_2$ , which affords the considerable increase in line widths, indicates restricted motion of the dye upon encapsulation. Assuming that intramolecular dipole–dipole relaxation is the predominant relaxation mechanism, the  $T_2/T_1$  ratio for free Reichardt's dye (in  $\text{CD}_3\text{OD}$ ) yields a correlation time  $\tau = 4.6 \times 10^{-10}$  s, consistent with the tumbling motions of a small molecule in solution. The  $T_2/T_1$  ratio for the encapsulated dye (in  $\text{D}_2\text{O}$ ) gave a correlation time  $\tau = 2.05 \times 10^{-9}$  s, which is consistent with the motions of the large dendrimer molecule. These correlations times correspond to the two sides of the  $T_1$  minimum, which is expected to occur at  $\tau \approx 1.9 \times 10^{-10}$  s at 500 MHz magnetic field strength.<sup>47</sup> Additionally, when the dye is encapsulated within the dendrimer, the succinic acid methylenes of [G4]-PGLSA-OH shifted upfield from 2.7 to 2.6 ppm as a consequence of the ring current effects associated with the aromatic rings of Reichardt's dye. The  $T_1$  relaxation time constant of the succinic acid protons also decreases slightly from 0.60 to 0.55 s.

$^1\text{H}$  NOESY spectra were recorded to explore the molecular interactions between the dendrimer and the encapsulated Reichardt's dye. Expansions of the aromatic and aliphatic regions are shown in Figures 5 and 6, respectively. Ring I shows strong intramolecular NOEs to rings III and IV, while rings II and V show weaker NOEs to the other aromatic rings. Moreover, a large number of intermolecular NOEs are also observed between the aromatic protons of Reichardt's dye and the methylenes of succinic acid and the methines and methylenes of glycerol, demonstrating significant close range dipolar interactions. Because the intramolecular distance between the

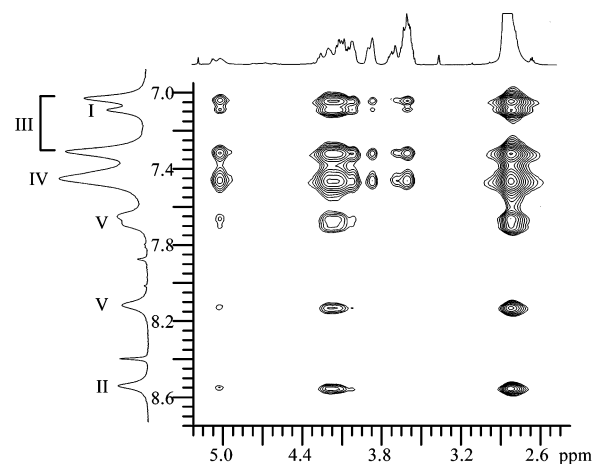


**Figure 6.** Aliphatic expansion of  $^1\text{H}$  NMR NOESY of [G4]-PGLSA-OH encapsulated Reichardt's dye in  $\text{D}_2\text{O}$ .

meta protons (3,5) in rings I and II of Reichardt's dye is approximately 3 Å, we estimate the intermolecular cross-peaks to indicate distances of 5 Å or less between the dye and the dendrimer. Furthermore, when the NOESY diagonal is phased negatively, the off-diagonal NOE cross-peaks from the dendrimer and encapsulated dye also phased negatively.<sup>48</sup> These data indicate that the association between the dye and dendrimer is sufficiently strong to observe dipolar through space NOE effects, and that the NOEs are associated with time scales typical of a large dendrimer macromolecule, confirming that the encapsulated dye molecule tumbles on approximately the same time scale as the dendrimer. The  $^1\text{H}$  NOESY spectra obtained for free Reichardt's dye (in  $\text{CD}_3\text{OD}$ ) are typical for small molecules.<sup>49</sup> When the NOE diagonal peaks are phased negative, all the off-diagonal cross-peaks for the free dye (in  $\text{CD}_3\text{OD}$ ) are positive, consistent with NOE behavior for a small molecule.

To investigate the potential drug delivery application with these dendritic macromolecules, the drug 10-hydroxycamptothecin (10HCPT) (**4**), a topoisomerase I inhibitor, was encapsulated within PGLSA dendrimers.<sup>50</sup> This poorly water soluble (6  $\mu\text{M}$ ) anticancer drug (Figure 1) has a different molecular weight ( $M_w = 364$  g/mol), shape, and electronic structure than Reichardt's dye. 10HCPT was encapsulated in the [G4]-PGLSA-COONa dendrimer at a concentration of 200  $\mu\text{M}$ . Initial attempts to encapsulate 10HCPT in [G4]-PGLSA-OH were not successful, as a precipitate formed upon standing. Thus, we encapsulated 10HCPT within the larger carboxylate terminated dendrimer, [G4]-PGLSA-COONa, which is more water soluble. The aromatic protons of the encapsulated 10HCPT are clearly visible and distinct from the dendrimer protons in the  $^1\text{H}$  NMR spectrum (Figure 7). 1D difference NOE spectra, with selective irradiation of the internal succinic acid protons (2.68 ppm), reveals NOE dipolar interactions to four of the five aromatic proton signals of 10HCPT (Figure 8). However, when the peripheral succinic acid protons (2.55 ppm) were irradiated, no selective NOEs were observed to the aromatic protons of 10HCPT. The NOEs to the internal succinic acid protons suggest the internalization of 10HCPT within the dendrimer.

(47) Dwek, R. *Nuclear Magnetic Resonance (NMR) Applications to Enzymatic Systems*; Oxford University Press: London, 1973.

(48) Wuthrich, K. *NMR of Proteins and Nucleic Acids*; John Wiley & Sons: New York, 1986.

(49)  $^1\text{H}$  NOESY spectra of free Reichardt's dye is available in the SI (SI Figure 3).

(50) Wani, M. C.; Wall, M. E. *J. Org. Chem.* **1968**, *34*, 1364–1367.

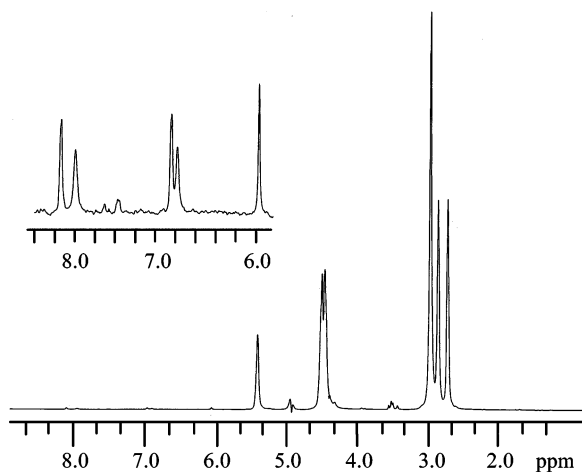


**Figure 7.**  $^1\text{H}$  NMR spectrum of 10HCPT encapsulated within [G4]-PGLSA-COONa ( $\text{D}_2\text{O}$ , ppm from DSS). Inset: Expansion of aromatic region, 1000-fold in vertical scale.

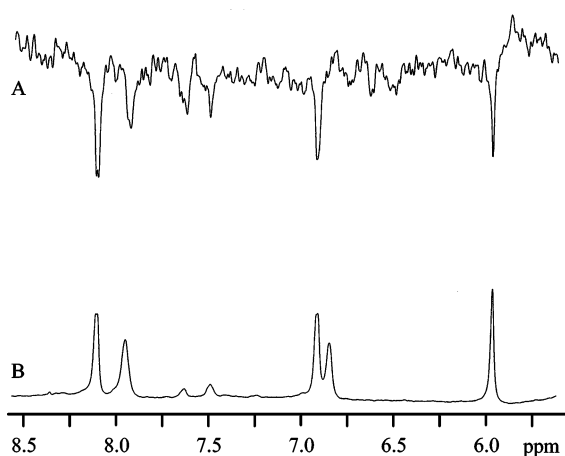


**Figure 8.** 1D  $^1\text{H}$  NOEs (A) between encapsulated 10HCPT (B) and interior succinic acid protons of [G4]-PGLSA-COONa.

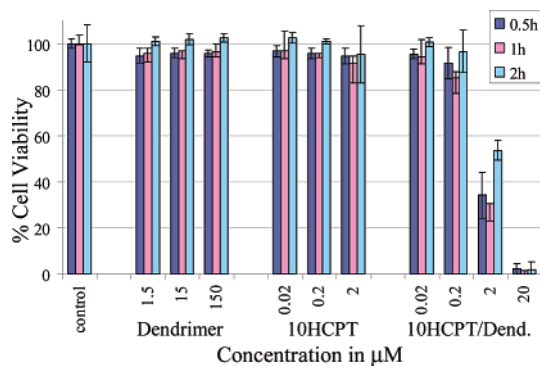


**Figure 9.** Cytotoxicity assay with human breast cancer, MCF-7, cells (5000 cells/well;  $n = 8$ ).

The anticancer activity of the encapsulated 10HCPT was evaluated using a standard NCI sulforhodamine B assay. Varying concentrations of [G4]-PGLSA-COONa encapsulated 10HCPT were incubated for 0.5 to 2 h with MCF-7 human breast cancer cells (5000 cells/well). Under these experimental conditions, no cytotoxic effects were observed with the dendrimer, whereas cell viability was significantly reduced in the presence of the encapsulated 10HCPT (Figure 9). The apparent lack of cytotoxicity with free 10HCPT is attributed to the high concentration of cells relative to the 10HCPT concentration.

At similar drug concentration, but lower cell concentration, cytotoxicity is observed with free 10HCPT (50% cell viability, data not shown). Additional cell studies examining cell and 10HCPT concentration dependence as a function of incubation time, as well as cell growth cycle, are ongoing and the results will be reported in a future publication. The highest concentration of encapsulated 10HCPT (20  $\mu\text{M}$ ) showed substantial cytotoxicity with less than 5% of the cells remaining viable. These *in vitro* results demonstrate that the anticancer activity of 10HCPT is retained after encapsulation within the dendrimer and that the dendrimer itself is a suitable delivery vehicle for hydrophobic anticancer drugs.

## Summary

The encapsulation of hydrophobic compounds within G4 dendrimers composed of succinic acid and glycerol is demonstrated. NMR studies reveal strong NOEs between the encapsulant and the dendrimer. Reichardt's dye and 10-hydroxycamptothecin, were successfully encapsulated suggesting that the dendrimer is a host for a range of structurally and electronically different hydrophobic molecules. The combined spectroscopic data portray a physical description where the dendrimer surrounds the encapsulant. The entrapment of a hydrophobic compound within the aliphatic dendrimer can be rationalized by the strong association between the encapsulant and the dendrimer, and the poor water solubility of the encapsulant. The solubility of the resultant dendrimer/encapsulant supramolecular assembly in water is attributed to the peripheral hydroxyl (or carboxylate) groups and the penetration of water molecules within the structure. The activity of the encapsulated 10HCPT was retained, as demonstrated by its cytotoxicity to human breast cancer cells. The results described herein provide further incentive for basic studies of dendritic macromolecules as well as the optimization of their macromolecular chemical and physical properties for specific medical applications.

**Acknowledgment.** This work was supported in part by the Pew Scholars Program in the Biomedical Sciences, the Johnson and Johnson Focused Giving Program, the Army Research Office, and the NIH (R01 EY13881). The Duke NMR Center is supported in part by NIH NCI P30-CA-14236 (A.A.R.). We thank Drs. G. Manikumar, N.H. Oberlies, and M.C. Wani of the Natural Products Laboratory at Research Triangle Institute for providing samples of 10-hydroxycamptothecin used in these studies. We also thank Lovorka Degoricija for help with the UV-vis experiments. C.E.I. thanks the National Research Council Associateship Program for a Postdoctoral Fellowship. M.W.G. also thanks the Dreyfus Foundation for a Camille Dreyfus Teacher-Scholar, the 3M corporation for a Non-Tenured Faculty Award, and the Alfred P. Sloan Foundation for a Research Fellowship.

**Supporting Information Available:** Detailed experimental information and characterization data. This material is available free of charge via the Internet at <http://pubs.acs.org>.